

DOI: 10.1002/adma.200602667

Length-Dependent Uptake of DNA-Wrapped Single-Walled Carbon Nanotubes**

By Matthew L. Becker,* Jeffrey A. Fagan, Nathan D. Gallant, Barry J. Bauer, Vardan Bajpai, Erik K. Hobbie, Silvia H. Lacerda, Kalman B. Migler, and John P. Jakupciak

Uncertainty over the potential detrimental effects of engineered nanomaterials on human health and the environment has fueled public debate and the push for additional regulatory oversight.^[1] For single-walled carbon nanotubes (SWNTs) the published data citing in vitro toxicity are particularly inconsistent and widely disputed.^[2–12] The underlying reasons for the discrepancies can be attributed to two causes: first, the wide variability in sample preparation and “purification” methods, including incomplete characterization of the SWNT materials following purification, such as minimal description about their post-purification solution behavior; and second, the use of nonuniform characterization methods and materials with different preparative protocols, viability assessment methods, and cell/species populations. Unfortunately, both points have rarely been addressed simultaneously in the literature and consequently have led to the wide variety of results. Even for well developed and optimized experimental protocols, insufficient characterization of samples makes identification of the toxic parameter(s) exceedingly difficult. Further complicating the elucidation of the physical properties causing in vitro and in vivo toxicity with SWNT materials is the wide distribution of tube diameters, lengths, and chiralities produced by current synthesis methods. Definitive discrimination of relative and synergistic effects with respect to these differences will continue to be impossible without implementation of precise measurements, complete characterization, and the use of well-defined materials.

One of the main sources of the variation in the published toxicity and biocompatibility data is the wide variability in SWNT dispersion, which results from many different preparative protocols and methods. While there is broad agreement that biological studies should put more emphasis on detailed characterization of test nanomaterials,^[6] the role of the disper-

sion state as a definitive factor influencing the cellular exposure and response to the SWNTs has often been ignored. Given a constant dosage, differences in dispersion ranging from macroscopic aggregates to micrometer-scale clusters, bundles of multiple nanotubes or individually dispersed nanotubes will dramatically affect the absolute size and amount of surface area of the nanotube material to which the cells are exposed. Our previous work has demonstrated that different SWNT preparation methods yield materials possessing varying degrees of dispersion, with one common result being networks of tubes that do not readily exchange once clustered.^[13,14] Notable, however, is the use of small molecule surfactants to induce SWNT solubility and dispersion in aqueous solutions. Dispersion protocols involving surfactants are attractive, as the incorporation of the nanotube inside a surfactant shell does not appreciably alter the graphitic structure and desirable physicochemical properties of the SWNTs.^[15] However, many surfactant dispersions are only partially effective at dispersing SWNT material, and thus yield suspensions of aggregates and not singly dispersed nanotubes.^[13] Recently, DNA, peptides, and carbohydrates have been used in this surfactant/wrapping polymer role and have been demonstrated to suspend SWNTs, with high individual dispersion of the nanotubes.^[13,16,17] These dispersions, in the case of DNA, are even stable enough to allow for separation of the dispersed material into well-defined subpopulations of the SWNTs.

Recent reports have highlighted successes in separating polydisperse SWNT populations into well-defined length and chirality fractions using gel chromatography,^[15,17,18] size exclusion chromatography (SEC),^[19–25] ion chromatography (IC),^[16,26,27] or various forms of electrophoresis.^[28–31] This sorting affords opportunities to explore which fractions and/or properties in particular are contributing to the cellular toxicity. Herein we describe our efforts in generating well-dispersed, separated-length fractions by SEC, the exhaustive characterization of these fraction populations, and high-concentration in vitro toxicity data, which indicate a threshold on the length and corresponding toxicity of SWNTs that are up-taken into cells.

Dispersion of SWNTs in aqueous solutions typically involves some detergent formulation and sonication protocol for both separating and suspending SWNT aggregates in solution. For our aqueous preparations, DNA wrapping was used as it imparts high-concentration solubility, successfully disperses individual SWNTs, and does not significantly alter the

[*] Dr. M. L. Becker, J. A. Fagan, N. D. Gallant, B. J. Bauer, V. Bajpai, E. K. Hobbie, S. H. Lacerda, Dr. K. B. Migler, J. P. Jakupciak
National Institute of Standards and Technology, Polymers Division
100 Bureau Drive, Gaithersburg, MD 20899-8543 (USA)
E-mail: mlbecker@nist.gov

[**] Research support from an NIST Innovation in Measurement Science Award for Carbon Nanotube Metrology and NIST/National Research Council postdoctoral fellowships (N.D.G. and J.A.F.) are gratefully acknowledged.

electronic structure of the SWNT. Centrifugation after DNA wrapping removes the vast majority of metal catalyst, bundled-SWNT fibers, and amorphous carbon chunks, yielding a well-dispersed distribution of SWNT lengths at concentrations of ca. 35–45 % of the original suspended mass.

In Figure 1A, the relative absorption spectra of the parent pre-centrifuge and post-centrifuge SWNT dispersions are shown. Of note is the difference in intensity and clarity of the absorption peaks due to SWNT optical transitions in the concentrated post-centrifuge dispersion compared to the initial pre-centrifuge SWNT suspension. Centrifugation appears to preferentially remove material that does not display the optical characteristics of dispersed SWNT material. Thus, the post-centrifuge dispersion is substantially purified, relative to the raw soot, and is ca. 85 % by mass SWNT material based on a rough estimate of ca. 55 % by mass initial purity.

A Wst-1 (see Experimental for definition) assay was used to look for reductions in metabolic activity (cell viability) of the cell populations upon exposure to the DNA-wrapped SWNTs. It was previously demonstrated that SWNTs do not directly interfere with the metabolic reduction of Wst-1.^[12] Serial dilutions of the concentrated post-centrifuge SWNT dispersion in

phosphate-buffered saline (PBS) were prepared and 10 μL added to 100 μL of culture media on adherent IMR90 human lung fibroblasts in a 96-well plate. Subsequently, the cells were incubated with the tubes for 16 h, prior to the Wst-1 assay. While this is significantly longer than the normal 2 h incubation period used in most small-molecule metabolic assays, this time frame is consistent with those listed in the literature for other SWNT bioassays.^[8,12] Photometric quantification was performed at 450 nm; the results are given in percent as relative values to the negative control, wherein the untreated (negative) control was set to be 100 % viable (Fig. 1B). The two highest solution concentration inoculations, 360 and 197 $\mu\text{g mL}^{-1}$, are significantly higher than we have found reported in the literature, and reduced cell viability by 75 % and 72 %, respectively. Concentrations below 20 $\mu\text{g mL}^{-1}$ did not significantly reduce cell viability. These cell viability measurements are consistent with the values found in the literature stating that metabolic inhibition occurs somewhere between 10 and 50 $\mu\text{g mL}^{-1}$. The exact *effective* solution concentrations of the literature inoculations are generally unknown, however, as measures of SWNT dispersion are rarely provided. The transmission electron microscopy (TEM) images (Fig. 1C

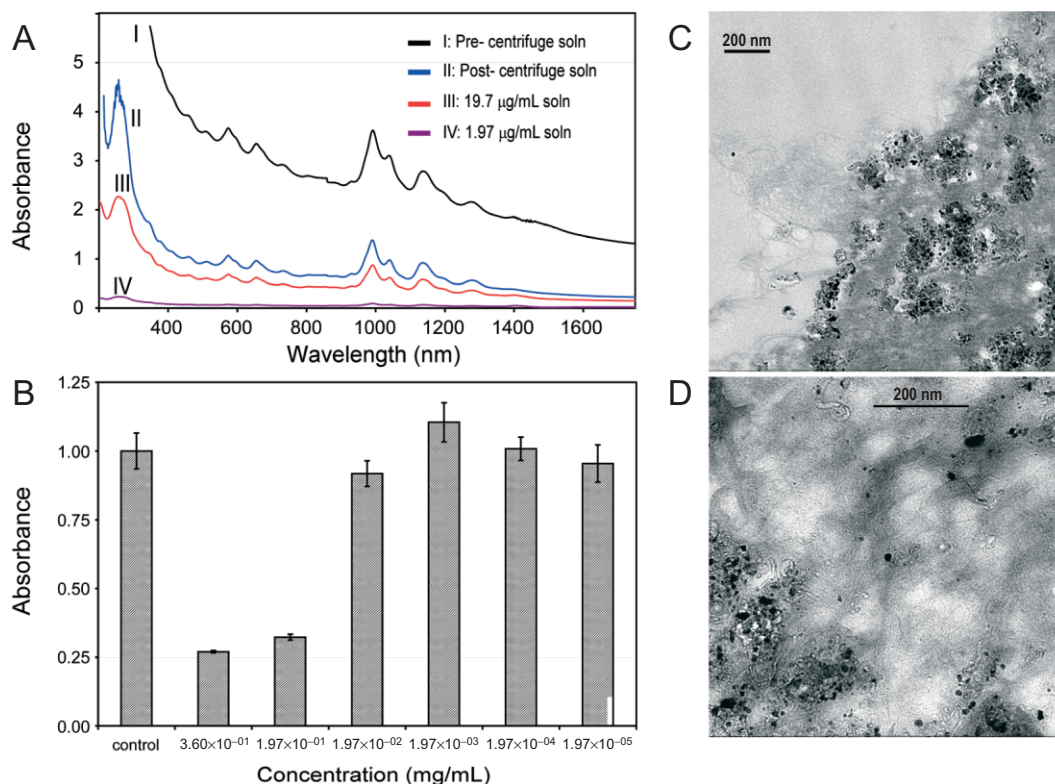


Figure 1. A) Comparison of absorption spectra for the pre-centrifuge, post-centrifuge, 19.7 $\mu\text{g mL}^{-1}$, and 1.97 $\mu\text{g mL}^{-1}$ samples of DNA-wrapped SWNTs. The pre-centrifuge spectra (black line) shows the absorbance of a (1.1 \pm 0.1) mg mL^{-1} as-mixed SWNT suspension. The centrifuged material retains the spectral features related to SWNTs apparent in the sonicated material and is, thus, partially purified by the DNA-dispersion process. B) The results of Wst-1 assay on IMR90 human lung fibroblast cells incubated for 16 h with DNA-wrapped SWNT at the defined concentrations. The two highest SWNT concentrations, 360 and 197 $\mu\text{g mL}^{-1}$, significantly inhibited the metabolic activity, while the lesser concentrations were insignificant from the control phosphate-buffered saline (PBS). C, D) Transmission electron microscopy (TEM) images of SWNTs incubated with cells and fixed in an epoxy matrix showing the longer tubes on the outside of the cell membrane (C) and the shorter tubes penetrating the membrane and residing in the cytosol (D).

and D), however, depict long tubes being excluded from the cell interior while the shorter SWNTs are able to access the cytosol.

Extraction of the supernatants (50 μL each) from the 96-well plates revealed that measurable quantities of the original tube populations remained in solution, indicating incomplete uptake of the SWNTs by the cells. While this was not surprising for the highest 360 and 197 $\mu\text{g mL}^{-1}$ inoculating concentrations (35 % and 27 % remaining in the supernatant), in which cell death may have occurred prior to all of the tube being internalized, approximately 32 % of the SWNT remained in solution for the 19.7 $\mu\text{g mL}^{-1}$ concentration. The viability loss of this fraction was statistically insignificant compared to the viability loss in the PBS controls, but after 16 h one might expect that most of the SWNT should have been consumed. Figure 2A shows a comparison of the absorbance of the (19.7 ± 0.15) $\mu\text{g mL}^{-1}$ inoculating SWNT solution to the absorbance of the SWNTs remaining in the supernatant after 16 h incubation (scaled for experimental dilution). For the 197 $\mu\text{g mL}^{-1}$ concentration, (27 ± 5) % of the SWNTs remained in the supernatant after incubation. Similar results for the percent of unconsumed nanotubes were found for the 19.7 $\mu\text{g mL}^{-1}$ and 1.97 $\mu\text{g mL}^{-1}$ inoculation concentrations. The percent of remaining SWNT absorbance is shown in Figure 2B for those concentrations at which the supernatant concentration was within measurement limits. The two sets of data correspond to measurements on the supernatant from those wells to which Wst-1 was added for measurement of the biological activity, and for a second set of wells to which the Wst-1 was not added. The point measured as retaining all of the SWNT absorbance for the inoculating concentration of 360 $\mu\text{g mL}^{-1}$ for the “Cells + Tubes only” repeat is likely due

to either overwhelming of the cells resulting in quick cell death and/or the release of the nanotubes upon cell death. This result suggests a selective rejection of certain SWNTs in the population by the cells, as the ratio of the consumed to inoculating concentration tubes is nearly invariant over several decades difference in absolute consumed mass. As no apparent difference in the relative uptake of different SWNT chiralities is observed (see Fig. 2A, inset), the data is consistent with a hypothesis of length-based selection/rejection of SWNTs by the cells.

Using SEC, the parent SWNT solution (9) was separated into multiple fractions. Twelve of the distinct fraction populations were collected and characterized. Using multiple runs, sufficient quantities were collected, which allowed for characterization as well as in vitro cell assessments at physiologically relevant concentrations. The dilute fractions, as well as parent solution, were concentrated and purified of free DNA using a forced air dialysis method that is able to concentrate the DNA-wrapped SWNTs solutions up to ca. 4 mg mL^{-1} without any apparent change in the dispersion quality. The concentrations and characterization data of the dispersed SWNT fractions rather than pre-centrifuged parent concentrations are listed in Table 1. These concentrations are relevant for metabolic-based in vitro toxicity testing, and the concentrations of the individual fractions are higher in most cases than previous unfractionated inoculations described in the literature. The radii of gyration (R_g) measurements, as collected from SEC, were converted to lengths using a multiplication factor for a rigid rod of $\sqrt{12}$.

Following characterization, Wst-1 experiments were performed on each on the length fractions. Briefly, 10 μL of each nanotube solution was added to IMR90 cells (50 μL ,

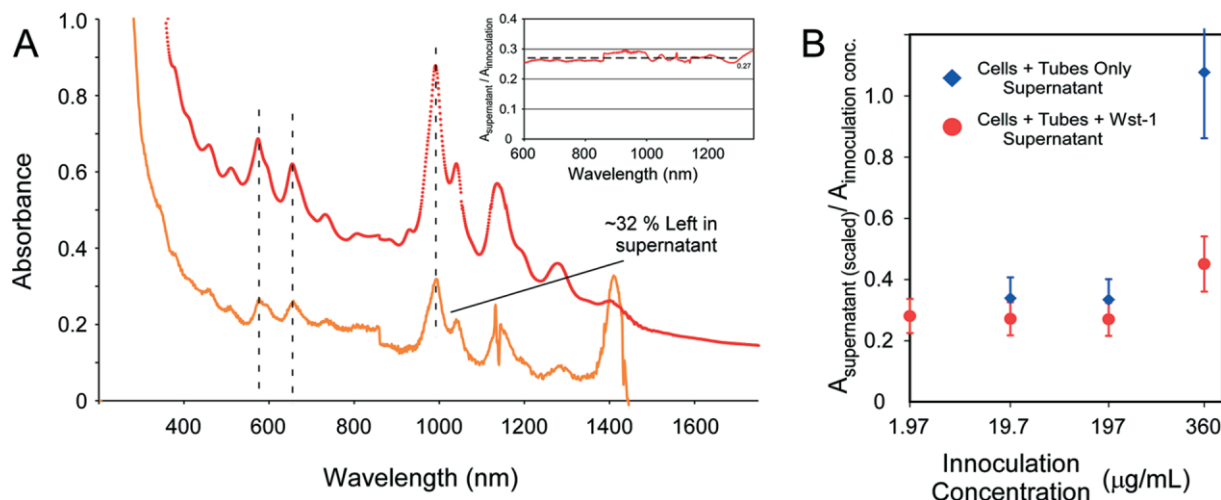


Figure 2. A) Comparison of the absorption spectra of the inoculating SWNT dispersion (red dots) to the (scaled for dilution) spectra of the removed supernatant (orange line) after 16 h for the 19.7 $\mu\text{g mL}^{-1}$ concentration. Approximately (32 ± 5) % of the SWNT absorbance remains in the solution. The inset shows that the removed amount of SWNTs is approximately constant regardless of SWNT chirality. B) Fraction of absorbance remaining in the SWNT–cell supernatant after 16 h relative to the inoculating concentration. The supernatant absorption was corrected for the intrinsic dilution of the experiment. The supernatant retained approximately 32 % of the absorbance of the inoculating solution over two decades change in the initial concentration. The two sets of data points correspond to measurements on the supernatant on those wells from which Wst-1 was added for measurement of the biological activity, and for a second set of wells to which the Wst-1 was not added.

Table 1. Summary of characterization data for individual length fractions (R_g : radius of gyration; AFM: atomic force microscopy).

Sample fraction	R_g (SEC) [nm]	Length (SEC) [nm]	Length (AFM) [nm]	Concentration [mg mL^{-1}]
1	113.5 ± 5.1	393 ± 18	–	0.031
2	96.8 ± 7.9	335 ± 27	367 ± 61	0.167
3	72.9 ± 7.4	253 ± 26	303 ± 11	0.180
4	54.6 ± 5.0	189 ± 17	210 ± 48	0.126
5	42.4 ± 3.4	150 ± 12	149 ± 43	0.266
6	34.7 ± 2.6	120 ± 9	138 ± 60	0.119
7	29.2 ± 2.0	101 ± 7	76 ± 27	0.191
8	25.8 ± 1.4	89 ± 5	–	0.134
9			distribution	

5000 cells) in 96-well plates. Following 16 h incubation, A_{450} measurements were collected for the purpose of background subtraction. Following background collection, 10 μL of Wst-1 solution was added to each well, and after a 2 h incubation period, A_{450} measurements were collected to assess cell viability. The longer fractions **2** and **3**, (335 ± 27) nm and (253 ± 26) nm, respectively, did not affect the viability of the cells. However, the shorter SWNT fractions did affect the viability at similar concentrations. Shown in Figure 3B is an absorbance versus concentration plot for each of the SWNT length fractions and their respective serial dilutions. However, all the length fractions shorter than **3** exhibited decreased metabolic activity at similar concentrations. Live–dead staining of the individual fractions at these concentrations showed that all cells below the dashed line were in fact dead after the allotted incubation times. The results suggest that the tube fractions retained in the supernatant were longer than (189 ± 17) nm. These results support the length-dependent uptake hypothesis and suggest that shorter tubes may therefore be more toxic to cells than longer SWNTs. Several different cell lines, including A549 (human alveolar basal epithelial cells), MC3T3-E1 (clonal murine calvarial), and A10 (embryonic rat thoracic aorta medial layer myoblasts) cells, were measured and exhibited similar results. We are confident that the results will be representative of a great number of additional cell lines. However, this list does not represent the full spectrum of cell types, and we expect that there will be exceptions that will not exhibit this length-dependent uptake behavior. Additional lines are being tested as sufficient materials are being produced. IMR90 cells were used specifically because they are the primary “normal lung fibroblasts” used in many different studies, characterized and adopted following the depletion of the WI-38 cell line.^[32] They have been thoroughly evaluated over the course of nearly three decades and have shown dose-dependent

toxicity behavior against small molecules and nanomaterials in the recent literature.

To confirm the preferential uptake data, we chose to incubate IMR90 cells with two length fractions, one above (**2**) and one below (**6**) the identified threshold, for identical time periods at concentrations below the measured toxicity limits. The SWNT sample **2** was labeled with Cy3-derivatized DNA and fraction **6** was labeled with Cy5-derivatized DNA. Following purification via dialysis and concentration, three separate cell experiments were preformed. Aliquots (30 μL) of the Cy3, Cy5 and an equal-volume mixture of Cy3 and Cy5 DNA-wrapped SWNTs were incubated for 16 h, fixed, and the cell

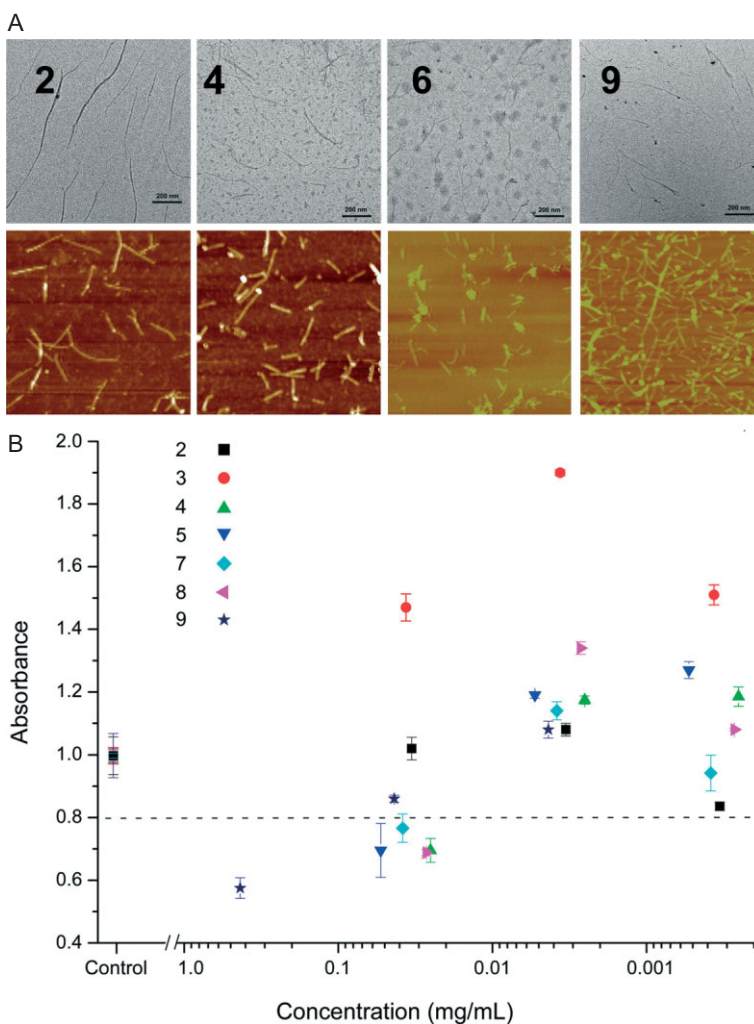


Figure 3. A) TEM (upper row) and atomic force microscopy (AFM) images (lower row) ($2 \mu\text{m} \times 2 \mu\text{m}$) of the parent centrifugation SWNT solution (**9**) and the individual length fractions of samples **2**, **4**, and **6**. The representative images collected using both TEM and AFM correlate well with the calculated values converted via the radius of gyration measurements using online light-scattering detectors. B) The plot of absorbance versus concentration from the Wst-1 assay on the parent SWNT and each of the fractions as a function of their respective serial dilutions. All fractions below the dashed lines were dead as viewed by fluorescence microscopy using a live–dead assay. The absorbance values have been normalized to the cell populations treated with PBS as a control. The error bars represent one standard deviation from the mean of quadruplicate experiments and are the estimates of the standard uncertainty.

membrane and nuclei were stained for visualization via fluorescence microscopy. As seen in the representative images compiled in Figure 4, sample **2** (I) is excluded from the interior of the cell while sample **6** (III) is clearly present in the cytoplasm. A mixture of samples **2** and **6** (II) confirmed that only sample **6** was present in the cytoplasm.

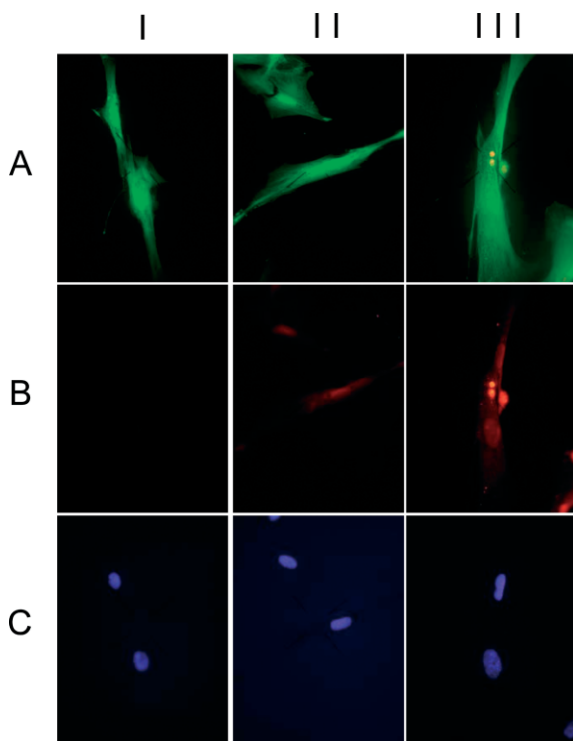


Figure 4. DNA end-functionalized with Cy3 and Cy5 were wrapped around SWNT fraction **2** (I) and **6** (III). IMR90 cells were incubated with each of the respective labeled length fractions and a 50:50 mix (II) of the two materials for 16 h at a concentration below the toxicity threshold. An Alexa-488 C2-maleimide labels the cytoskeleton (A), (B) indicates the absence or presence of the DNA-wrapped SWNTs and (C) is a DAPI nuclear stain. These representative images clearly indicate that the longer sample **2** is excluded while the shorter sample **6** is able to access the cell interior.

In summary, the viability of IMR90 human fibroblast cells was measured via a Wst-1 assay for inoculation with high concentrations of individually dispersed DNA-wrapped single-walled carbon nanotubes. Concentrations of the broad-length-distribution dispersed SWNTs were found to induce dramatic reduction of viability in the IMR90 cells above the 20–25 $\mu\text{g mL}^{-1}$ concentration regime. Furthermore, a large and nearly constant percentage of each inoculating concentration was found to remain in solution regardless of the absolute inoculated mass. Spectroscopic measurement of the remaining material and further viability assays conducted with highly concentrated length populations indicate a length-selective uptake of nanotubes by the cell populations. The assays determined an approximate uptake threshold of approximately (189 \pm 17) nm, indicating that nanotubes shorter than this

length are consumed and likely induce more toxicity. A size threshold for preferential uptake is not a new concept in nanometer-scale materials, as size and surface-chemistry effects have been shown to influence cell uptake, retention, and biodistribution in other nanoparticle systems^[33–35] and have been suggested for multi-walled carbon nanotubes.^[36] The conclusions outlined in this Communication are obtained from DNA-wrapped materials exclusively. The coating or “wrapping material” used to suspend or disperse the SWNTs in aqueous media greatly influences the results. We have previously evaluated several types of dispersing agents including butyl grafting, surfactants, and polymer wrapping. However, after measuring the SWNT dispersion afforded by many of the respective methods found in the literature, we concluded that the results can not be compared. DNA wrapping offers superior dispersion compared to other suspension or dispersion methods, prohibiting an “equivalent” side-by-side comparison of mechanistic biobehavior or toxicity with different wrapping methods. We believe that length-dependent uptake may be a general phenomenon; however, it is important to note that, like other in vitro experiments, the exact threshold is expected to vary with cell type.

Experimental

Note: Certain equipment and instruments or materials are identified in the paper to adequately specify the experimental details. Such identification does not imply recommendation by the National Institute of Standards and Technology, nor does it imply the materials are necessarily the best available for the purpose.

SWNT Preparation: Aqueous dispersions of SWNTs were generated using the method of Zheng et al. described previously [16]. Briefly, single-walled “CoMoCat” SWNTs from Southwest Nanotechnologies (Batch NI6-A001) were sonicated (0.32 cm tip sonicator, Thomas Scientific) in a salt solution (0.2 mol L⁻¹ NaCl, 0.1 mol L⁻¹ tris(hydroxymethyl)aminomethane (Tris), 5 mmol L⁻¹ NaN₃ buffered to pH7 with HCl) in the presence of 30-mer 5'-GT(GT)₁₃GT-3' single-stranded DNA (Integrated DNA Technologies). SWNT powder and DNA were both loaded at (1.0 \pm 0.25) mg mL⁻¹. In all cases the sonication was performed in a 15 mL centrifuge tube immersed in an ice bath and tightly covered to reduce evaporation. The sonication period was 2 h at 9 W of applied power. Four batches were prepared in this manner and then mixed to produce a single batch of concentration (1.1 \pm 0.1) mg mL⁻¹. Post-sonication, the mixed suspension was further processed by centrifugation at 21 000 g_n in 1.5 mL centrifuge tubes for 2 h; the resulting supernatant is a stable, rich black liquid containing well-dispersed SWNT material. For the length-fractionated cell experiments, stock solutions of fluorescently labeled DNA (Integrated DNA Technologies) were generated by dissolution of the solid DNA with 18 M Ω cm⁻¹ water to a final concentration of 1 mg mL⁻¹ DNA. DNA-wrapped SWNT length fractions **2** and **6** were mixed (10 μ L) with 90 μ L of the Cy3- and Cy5-labeled DNA solutions, respectively. The mixed solutions were incubated at room temperature, in the dark, for 240 h. The solutions were subsequently concentrated using a forced air dialysis cell (Amicon) with a membrane molecular weight cutoff (MWCO) size of 30 000 Da to yield a higher concentration for inoculation into the well plate. Conveniently, the unattached DNA remaining in the solution was removed during the forced dialysis process.

Concentration Determination: Ultraviolet–visible–near-infrared (UV-vis-NIR) absorption spectroscopy was used to determine the concentration of SWNTs in solution at various stages in the experi-

ment. Spectroscopy was performed in transmission mode on a Perkin–Elmer Lambda 950 UV-vis-NIR spectrophotometer over the wavelength range of 1750–190 nm. In all cases, the incident light was depolarized prior to the sample compartment, and the instrument was corrected for both the dark current and background spectra; data were recorded at 1 nm increments, with an instrument integration time of 0.2 s per increment. In all cases the reference beam was left unobstructed, and the subtraction of the appropriate reference sample was performed during data reduction. Calibration of the SWNT concentration in solution was calculated by relation to the absorbance of the original 1.1 mg mL⁻¹ SWNT suspension at 903 nm. For concentrated samples, absorption spectra were also recorded on volumetric dilutions within the linear Beer–Lambert regime for relating the concentration to absorbance; undiluted concentration was determined by extrapolation from the diluted sample. The final concentration of the stock dispersion by this measure was (2.17 ± 0.15) mg mL⁻¹ [37].

Size Exclusion Chromatography (SEC): Length separation was achieved by SEC using a Waters Delta 600 pump, Waters 2996 UV-vis photodiode array, and a Wyatt Dawn EOS multi-angle light-scattering detector with a SepaxCNT (SEC-2000 + SEC-1000 + SEC-300) column set [25]. A centrifuged, but unconcentrated, SWNT dispersion, prepared as above, was filtered through a 0.45 μm filter and injected in 0.5 mL increments; the flow rate of the aqueous mobile phase (0.2 mol L⁻¹ NaCl, 0.04 mol L⁻¹ Tris, 200 ppm Na₃ buffered to pH 7 with HCl) was 0.5 mL min⁻¹. Samples were collected at 2 min intervals and eight duplicate runs were performed. Radius of gyration was calculated using Wyatt Astra software.

Transmission Electron Microscopy (TEM): TEM of carbon nanotubes was performed on a Philips EM 400T microscope operating at 120 kV equipped with a Soft Imaging System charge-coupled device (CCD) camera (Cantega 2 K). TEM samples were prepared by dropping dialyzed and diluted solutions of SWNTs and length fractions in water onto 600-mesh, mica-loaded, carbon-coated copper grids, which were then liquid-nitrogen quenched and immediately lyophilized.

Atomic Force Microscopy (AFM): Tapping-mode AFM measurements were conducted in air using a Nanoscope IV system (Digital Instruments) operated under ambient conditions with standard silicon tips (NanoDevices Metrology Probes; length, *L*, 125 μm; normal spring constant, 40 N m⁻¹; resonance frequency, 280–330 kHz). Briefly, the solutions were diluted 100× in water (18 MΩ cm⁻¹) prior to being deposited (2 μL) onto plasma-cleansed Si wafers or freshly cleaved mica. After being allowed to dry, any residual salt was washed away by a water deposition/wicking procedure ≈ 2–3 times to afford clear imaging conditions.

Cell Culture: A diploid primary human fibroblast adherent cell line, derived from fetal lung tissue IMR90 (ATCC, CCL-186), was obtained from American Type Culture Collection (ATCC, Rockville, MD). Cells were cultured in Dulbecco's modified Eagle's medium (DMEM) containing 4.5 mg mL⁻¹ glucose, 10% (by volume) heat-inactivated fetal calf serum (FCS), 2 mmol L⁻¹ L-glutamine, 50 μg mL⁻¹ penicillin, and 100 Units mL⁻¹ streptomycin. The cells were grown in a humidified incubator at 37 °C (95% room air, 5% CO₂). Prior to the viability experiments on the parent SWNTs, the cells were seeded into 96-well plates at 50 000 cells mL⁻¹ (5000 cells/100 μL/well) and the respective SWNT fractions were seeded (2000 cells/40 μL/well) and incubated overnight. IMR90 cells were used specifically because they are the primary "normal lung fibroblasts" used in many different studies, following the depletion of the VA13 cell line, and have been thoroughly evaluated over the course of nearly 30 years, showing dose-dependent toxicity behavior against small molecules and other nanomaterials in the recent literature [38–40]. The length-fraction experiments involved 30 μL of each solution incubated in a six-well plate for the incubation conditions listed above. Slide preparation employed standard fixation and washing conditions, and three fluorescence images were captured: 1) a green-channel image for Alexa-488 C₂-maleimide-stained cell bodies; 2) a blue-channel image of DAPI-stained cell nuclei; 3) two separate red channels for the labeled DNA-wrapped SWNTs.

Wst-1 Assay: The tetrazolium salt 2-(4-iodophenyl)-3-(4-nitrophenyl)-5-(2,4-disulfophenyl)-2H-tetrazolium (Dojindo), better known as Wst-1, was used to detect a loss in viability upon cell-population exposure to SWNTs. Serial dilutions in phosphate-buffered saline (PBS) were made for each of the SWNT parent populations and SEC-sorted length fractions, and 10 μL of the respective SWNT concentration in PBS was added to the cell suspensions. Photometric quantification was performed at 450 nm (A₄₅₀) in an M5 Molecular Devices microplate reader. The experimental data were performed in triplicate or quadruplicate. The results are given as relative values [%] to the negative control, where the untreated (negative) control was set to be 100% viable.

Quantifying SWNT Retention: After incubation, 50 μL of supernatant was carefully removed from each well of the cell plate and retained. To measure the amount of nanotubes retained in the supernatant, 50 μL of deionized water was added to each well of the retained supernatant, and the liquid from each of these duplicate wells for the respective concentrations were combined. This was required to obtain an amount of liquid suitable for the UV-vis-NIR spectroscopy.

Received: November 22, 2006

Revised: January 22, 2007

- [1] V. L. Colvin, *Nat. Biotechnol.* **2003**, *22*, 1166.
- [2] D. B. Warheit, B. R. Laurence, K. L. Reed, D. H. Roach, G. A. M. Reynolds, T. R. Webb, *Toxicol. Sci.* **2004**, *77*, 117.
- [3] G. Jia, H. Wang, L. Yan, X. Wang, R. Pei, T. Yan, Y. Zhao, X. Guo, *Environ. Sci. Technol.* **2005**, *39*, 1378.
- [4] J. C. Carreor-Sanchez, A. L. Elias, R. Mancilla, G. Arrellin, H. Terrones, J. P. Laclette, M. Terrones, *Nano Lett.* **2006**, *6*, 1609.
- [5] H. Dumortier, S. Lacotte, G. Pastorin, R. Marega, W. Wu, D. Bonifazi, J.-P. Briand, M. Prato, S. Muller, A. Bianco, *Nano Lett.* **2006**, *6*, 1522.
- [6] R. H. Hurt, M. Monthieux, A. Kane, *Carbon* **2006**, *44*, 1028.
- [7] C.-W. Lam, J. T. James, R. McCluskey, S. Arepalli, R. L. Hunter, *Crit. Rev. Toxicol.* **2006**, *36*, 189.
- [8] A. Magrez, S. Kasas, V. Salicio, N. Pasquier, J. W. Seo, M. Celio, S. Catsicas, B. Schwaller, L. Forro, *Nano Lett.* **2006**, *6*, 1121.
- [9] S. K. Smart, A. I. Cassady, G. Q. Lu, D. J. Martin, *Carbon* **2006**, *44*, 1034.
- [10] C. M. Sayes, F. Liang, J. L. Hudson, J. Mendez, W. Guo, J. M. Beach, V. C. Moore, C. D. Doyle, J. L. West, W. E. Billups, K. B. Ausman, V. L. Colvin, *Toxicol. Lett.* **2006**, *161*, 135.
- [11] D. B. Warheit, *Carbon* **2006**, *44*, 1064.
- [12] J. M. Worle-Knirsch, K. Pulskamp, H. F. Krug, *Nano Lett.* **2006**, *6*, 1261.
- [13] B. J. Bauer, E. K. Hobbie, M. L. Becker, *Macromolecules* **2006**, *39*, 2637.
- [14] H. Wang, W. Zhou, D. L. Ho, K. I. Winey, J. E. Fischer, C. J. Glinka, E. K. Hobbie, *Nano Lett.* **2004**, *4*, 1789.
- [15] W. I. Zhou, M. F. Islam, H. Wang, D. L. Ho, A. G. Yodh, K. I. Winey, J. E. Fischer, *Chem. Phys. Lett.* **2004**, *384*, 185.
- [16] M. Zheng, A. Jagota, E. D. Semke, B. A. Diner, R. S. McLean, S. R. Lustig, R. E. Richardson, N. G. Tassi, *Nat. Mater.* **2003**, *2*, 338.
- [17] D. A. Heller, R. M. Mayrhofer, S. Baik, Y. V. Grinkova, M. L. Usrey, M. S. Strano, *J. Am. Chem. Soc.* **2004**, *126*, 14 567.
- [18] C. A. Dyke, M. P. Stewart, J. M. Tour, *J. Am. Chem. Soc.* **2005**, *127*, 4497.
- [19] D. Chattopadhyay, S. Lastella, S. Kim, F. Papadimitrakopoulos, *J. Am. Chem. Soc.* **2002**, *124*, 728.
- [20] G. S. Duesberg, W. Blau, H. J. Byrne, J. Muster, M. Burghard, S. Roth, *Synth. Met.* **1999**, *103*, 2484.
- [21] G. S. Duesberg, J. Muster, V. Krstic, M. Burghard, S. Roth, *Appl. Phys. A* **1998**, *67*, 117.
- [22] E. Farkas, M. E. Anderson, Z. H. Chen, A. G. Rinzier, *Chem. Phys. Lett.* **2002**, *363*, 111.

- [23] M. Holzinger, A. Hirsch, P. Bernier, G. S. Duesberg, M. Burghard, *Appl. Phys. A* **2000**, *70*, 599.
- [24] S. Niyogi, H. Hu, M. A. Hamon, P. Bhowmik, B. Zhao, S. M. Rozenzhak, J. Chen, M. E. Itkis, M. S. Meier, R. C. Haddon, *J. Am. Chem. Soc.* **2001**, *123*, 733.
- [25] X. Y. Huang, R. S. McLean, M. Zheng, *Anal. Chem.* **2005**, *77*, 6225.
- [26] S. R. Lustig, A. Jagota, C. Khripin, M. Zheng, *J. Phys. Chem. B* **2005**, *109*, 2559.
- [27] M. Zheng, A. Jagota, M. S. Strano, A. P. Santos, P. Barone, S. G. Chou, B. A. Diner, M. S. Dresselhaus, R. S. McLean, G. B. Onoa, G. G. Samsonidze, E. D. Semke, M. Usrey, D. J. Walls, *Science* **2003**, *302*, 1545.
- [28] R. Krupke, F. Hennrich, H. von Lohneysen, M. M. Kappes, *Science* **2003**, *301*, 344.
- [29] S. K. Doorn, R. E. Fields, H. Hu, M. A. Hamon, R. C. Haddon, J. P. Selegue, V. Majidi, *J. Am. Chem. Soc.* **2002**, *124*, 3169.
- [30] D. A. Heller, R. M. Mayrhofer, S. Baik, Y. V. Grinkova, M. L. Usrey, M. S. Strano, *J. Am. Chem. Soc.* **2004**, *126*, 14567.
- [31] S. K. Doorn, M. S. Strano, M. J. O'Connell, E. H. Haroz, K. L. Rialon, R. H. Hauge, R. E. Smalley, *J. Phys. Chem. B* **2003**, *107*, 6063.
- [32] W. W. Nichols, D. G. Murphy, V. J. Cristofalo, L. H. Toji, A. E. Greene, S. A. Dwight, *Science* **1977**, *196*, 60.
- [33] C. M. Pitsillides, E. K. Joe, X. Xunbin Wei, R. R. Anderson, C. P. Lin, *Biophys. J.* **2003**, *84*, 4023.
- [34] X. K. Sun, R. Rossin, J. L. Turner, M. L. Becker, M. J. Joralemon, M. J. Welch, K. L. Wooley *Biomacromolecules* **2005**, *6*, 2541.
- [35] S. M. Moghimi, A. C. Hunter, J. C. Murray, *Pharmacol. Rev.* **2001**, *53*, 283.
- [36] Y. Sato, Y. Yokoyama, K. Shibata, Y. Akimoto, S. Ogino, Y. Nodasaka, T. Kohgo, K. Tamura, T. Akasaka, M. Uo, K. Motomiya, B. Jeyadevan, M. Ishiguro, R. Hatakeyama, F. Watari, K. Tohji, *Mol. Biosyst.* **2005**, *1*, 176.
- [37] Uncertainties reported in this contribution reflect one standard deviation calculated by common methodology.
- [38] T. Zhang, J. L. Stilwell, D. Gerion, L. Ding, O. Elboudwarej, P. A. Cooke, J. W. Gray, A. P. Alivasatos, F. F. Chen, *Nano Lett.* **2006**, *6*, 800.
- [39] J. Du, D. H. Daniels, C. Asbury, S. Venkataraman, J. Liu, D. R. Spitz, *J. Biol. Chem.* **2006**, *281*, 37416.
- [40] C. Cecchi, A. Pensalfini, S. Baglioni, C. Fiorillo, R. Caporale, L. Formigli, G. Liguri, M. Stefani, *FEBS J.* **2006**, *273*, 2206.